ESTIMATION OF LAND SURFACE TEMPERATURE USING LANDSAT-7 ETM+ THERMAL INFRARED AND WEATHER STATION DATA

Jiansheng Yang and Y.Q. Wang
Department of Natural Resources Science
University of Rhode Island
Kingston, RI 02881, USA
jyan1185@postoffice.uri.edu, yqwang@uri.edu

Abstract

A simple regression calibration model was developed in this study to estimate the land surface temperature using Landsat Enhanced Thematic Mapper plus (ETM+) thermal band combined with classification-based surface emissivity and solar zenith angle. The brightness temperatures derived from satellite thermal data for 15 weather stations in southeast New England area were calibrated by the ground truth temperatures observed while the Landsat-7 overpasses. The surface emissivity was derived from the conventional image classification and solar zenith angle was calculated from station latitude and date and time of the observations. The correlation between the land surface temperature and brightness temperature was increased significantly after the surface emissivity and solar zenith angle were added to the model. The determination of coefficient (R^2) increased from 0.33 to 0.85. This indicates that the Landsat ETM+ thermal infrared data can be reasonably calibrated if appropriate ground truth and ancillary data are available.

1. Introduction

Land surface temperature (LST), controlled by the surface energy balance, atmospheric state, thermal properties of the surface, and subsurface mediums, is an important factor controlling most physical, chemical, and biological processes of the Earth (Becker and Li, 1990). In spite of the great importance in modeling and application of LST, confusions exits in both the use of the term and its determination with satellite thermal data. Numerous factors need to be quantified in order to assess the accuracy of the LST retrieval from satellite thermal data, including sensor radiometric calibrations (Wukelic *et al*., 1989), atmospheric correction (Cooper and Asrar, 1989), surface emissivity correction (Norman *et al*., 1990), characterization of spatial variability in land cover, and the combined effects of viewing geometry, background, and fractional vegetative cover. In estimation of LST from satellite thermal data, the digital number (N_D) of image pixels needs to be converted into spectral radiance using the sensor calibration data (Markham and Barker, 1986). However, the radiance converted from digital number does not represent a true surface temperature but a mixed signal or the sum of different fractions of energy. These fractions include the energy emitted from the ground, upwelling radiance from the atmosphere, as well as the downwelling radiance from the sky integrated over the hemisphere above the surface. Therefore, the effects of both surface emissivity and atmosphere must be corrected in the accurate estimation of LST.

The methods that are popularly used in correction of satellite observations of surface radiance for atmospheric effects fall into two categories, the direct methods which use atmospheric soundings of temperature and moisture from balloon-borne sonde, and the indirect approaches which attempt to accomplish atmospheric corrections with satellite observations only (Norman *et al*., 1995). Direct methods combine *in situ* measurements of temperature and moisture with atmospheric radiative transfer models, such as LOWTRAN and MODTRAN, which calculate the atmospheric transmittance and path radiance as a function of wavelength (Schott and Volchok, 1985; Goetz *et al*., 1995). Indirect methods derive vertical soundings of the atmosphere

from satellite observations and use atmospheric radiative transfer models. In addition, split-window algorithms using channels 4 and 5 of the NOAA Advanced Very High Resolution Radiometer (AVHRR) satellite instrument (Becker and Li, 1990), or channels 31 and 32 of NASA Earth Observing System Moderate Resolution Imaging Spectrometer (EOS/MODIS) (Vidal, 1991) have been widely applied in the atmospheric and emissivity correction of LST for different purposes. After proper corrections, LST can be computed from corrected radiance by reverse analysis of the Planck equation theoretically. However, in real application, such models are usually difficult to apply due to its sparse resolution and requirements of diverse variables.

Table 1. Seasonal mean emissivities for different 'emissivity classes' in MODIS band 31 and 32 (Snyder *et al*., 1998).

Emissivity Classes	Mean Emissivity (ε)					
	Green Season			Senescent Season		
	10.8-11.3μm	11.8-12.3μm	Average	10.8-11.3μm	11.8-12.3μm	Average
Needle Forest	0.989	0.991	0.990	0.986	0.988	0.987
Broadleaf Forest	0.987	0.990	0.989	0.968	0.971	0.970
Woody Savanna	0.988	0.991	0.990	0.975	0.978	0.977
Grass Savanna	0.987	0.991	0.989	0.973	0.975	0.974
Sparse Shrubs	0.972	0.975	0.974	0.970	0.976	0.973
Water/Wetland	0.991	0.986	0.989	0.991	0.986	0.989
Organic Bare Soil	0.977	0.982	0.980	0.977	0.982	0.980
Arid Bare Soil/ Urban	0.966	0.972	0.969	0.966	0.972	0.969

Little success has been done in the retrieval of LST from Landsat Thematic Mapper (TM) and ETM+ thermal data. TM/ETM+ has one thermal infrared band (10.44-12.42 μm), which makes the use of general split-window correction algorithm impossible, but the high spatial resolution (120 m for TM and 60 m for ETM+) are much attractive in the local and regional thermal infrared study. Some effects have been made on the retrieval of LST from Landsat 4 and 5 thermal infrared data in the past decade (Schott and Volchol, 1985; Wukelic *et al*., 1989; Goetz *et al*., 1995). The comparison among different algorithms in estimation of LST from TM data (Sospedra *et al*., 1998) shows that although the algorithms of Wukelic *et al*. (1989) and Goetz *et al*. (1995) are in relatively poor performance over a wide temperature range, they have the advantage of using only two parameters. On the other hand, Singh's (1988) method performs well with errors below 0.1 K, but six parameters are required in the model. Thus, it is desirable to develop new algorithms that can achieve a high accuracy in prediction of LST from TM/ETM+ thermal data with fewer parameters.

Surface emissivity is known to be one important factor in radiance balance and transfer. However, the Earth's surface is comprised of complicated land-use and land-cover types and the surface emissivities are difficult to measure accurately. Recently, a more detailed 'emissivity classification' was conducted by Snyder *et al*. (1998) based on the conventional land cover classification and dynamic and seasonal factors using MODIS thermal infrared bands. Therefore, each pixel in the thermal image can be classified as one of thirteen 'emissivity classes' according to the conventional land cover classification results (Table 1). Another important factor affecting the radiance emitted from surface or the surface temperature is incoming solar radiation at the Earth's surface. It is the result of a complex interaction of energy between the atmosphere and the surface (Dubayah and Rich, 1995).

By a statistical model that relates ground truth temperature with satellite brightness temperature, surface emissivity, and incoming solar radiation, it is possible to generate a correction algorithm, which has broader application potentials. The objective of this study is to

retrieve the LST by calibration of the brightness temperature obtained from Landsat-7 ETM+ thermal infrared data using surface emissivity based on the conventional classification and incoming solar radiation represented by the solar zenith angle.

2. Method

2.1 Study Area and Data

One scene of Landsat ETM+ image acquired on October 27, 1999 (path 12/row 31) was applied in this study. This scene covers the areas of the southern New England states, including part of Massachusetts, Connecticut, and the entire state of Rhode Island. The ETM+ scene was applied as the satellite data source and the corresponding area as the study area (Figure 1). Measurements of ground truth temperature (T_G) from 15 weather stations in this area concurrent with the time of the ETM+ data acquisition were retrieved from National Climate Data Center (NCDC). The digital numbers of ETM+ band-6 for the 15 weather stations were derived to estimate brightness temperature (T_B). Surface emissivities for each station were retrieved from conventional land cover classification of the ETM+ multispectral image. The solar zenith angles (θ), the replacement of incoming solar radiation, for each station were calculated using the latitude of the station and the date and time of the satellite observations.

2.2 Analysis

A GIS point coverage of the fifteen weather stations was generated and projected to the State Plane coordinate system (NAD83) in ESRI Arc/Info system. The ETM+ band-6 image was re-projected to the same map coordinates in ERDAS Imagine software system. Both the image file and point coverage file were then converted into grid format in Arc/Info. The digital numbers of the pixels corresponding to the location of the weather stations were retrieved using Spatial Analyst, one of the ESRI ArcView extensions. Retrieved digital numbers were then converted into spectral radiance using the following equation (Markham and Barker, 1986):

$$L_\lambda = 0.0056322 \times DN + 0.1238 \quad (1)$$

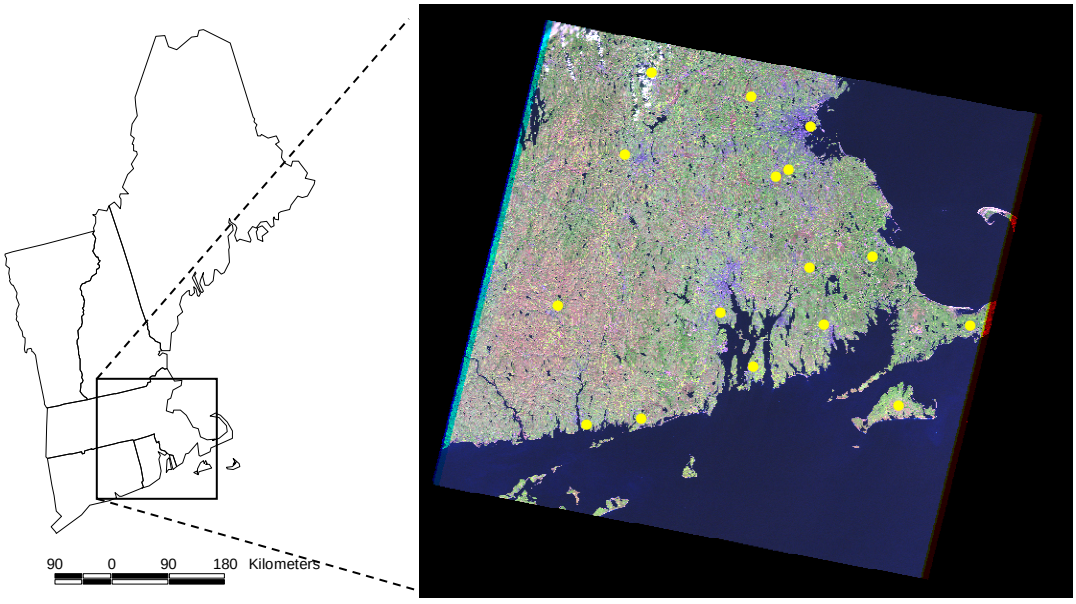

Figure 1. Study area, Landsat ETM+ image (path12/row31) with band combination RGB=543 for the study area, and the weather stations.

Finally, spectral radiances were converted into satellite brightness temperature using the following relationship that is similar to the Planck equation with two free parameters (Schott and Volchok, 1985; Wukelic *et al*., 1989):

$$T_B = \frac{K_2}{\ln\left(\frac{K_1}{L} + 1\right)} \tag{2}$$

where L the blackbody radiance for a temperature, T_B, integrated over the TM band-6, and K_1 and K_2 are two free parameters with the values of K_1= 60.776 mWcm^{-2}sr^{-1}μm^{-1}, K_2=1260.56 K

The hourly surface temperatures (T_G) observed on the ground stations at the time of Landsat-7 overpass were retrieved from NCDC Local Climatological Data Set.

Both unsupervised and supervised classification methods were applied to classify the ETM+ multispectral image to land-cover map and to derive associated surface emissivity. In unsupervised classification, 30 clusters were applied to assist the selection of training sites. The land cover classification system developed by the International Geosphere- Biosphere Program (IGBP) (Snyder *et al*., 1998) were applied to define the land cover types and guided the supervised classification using the *Maximum Likelihood* algorithm. After the classification, a post-classification recoding was applied to group the land cover types into eight broad emissivity classes, *i.e*., *Needle forest, Broadleaf forest, Woody, Shrub, Grass, Water, Organic bare soil, and Arid bare soil*, to determine the surface emissivity from Table 1.

A solar-zenith-angle calculator (Fitzpatrick and Stephens, 1995) was used to calculate the solar zenith angle using the latitude of each station, the date of ETM+ data acquisition, and the local time of the ETM+ observation.

Finally, a quadratic regression model of ground truth temperature against satellite brightness temperature, surface emissivities, and solar zenith angle was established.

3. **Results**

Surface 'emissivity classes' derived from image classification, digital numbers (N_D) derived from ETM+ thermal data and converted brightness temperatures (T_B), ground truth temperature (T_G) retrieved from NCDC, and calculated solar zenith angles (θ) for all 15 weather stations are summarized in Table 2.

Table 2. Fifteen weather stations and derived parameters.

Location	State	Lat.	Long.	Emissivity Classes	N_D	T_B(F)	T_G(F)	θ
Windham	CT	41.74	-72.18	Green Woody	124	66.00	57	68.88
Bedford	MA	42.47	-71.29	Green Shrubs	122	64.35	52	69.38
Gen Logan	MA	42.36	-71.01	Green Shrubs	121	63.52	53	69.30
Fitchburg	MA	42.55	-71.76	Arid Bare Soil	123	65.17	52	69.43
Barnstable	MA	41.67	-70.28	Green Forest	121	63.52	54	68.83
Marthas	MA	41.39	-70.62	Green Forest	126	67.64	56	68.65
Blue Hill	MA	42.21	-71.12	Green Forest	119	61.84	51	69.20
New Bedford	MA	41.68	-70.96	Green Grass	123	65.17	57	68.84
Norwood	MA	42.19	-71.17	Organic Bare Soil	122	64.35	55	69.19
Plymouth	MA	41.91	-70.73	Green Shrubs	121	63.52	53	69.00
Taunton	MA	41.88	-71.02	Arid Bare Soil	122	64.35	57	68.97
Worcester	MA	42.27	-71.88	Arid Bare Soil	120	62.69	51	69.24
Newport	RI	41.53	-71.28	Green Grass	121	63.52	59	68.74
Theo Francis	RI	41.72	-71.43	Green Shrubs	122	64.35	57	68.87
Westerly	RI	41.35	-71.80	Organic Bare Soil	123	65.17	60	68.62

Comparison between the original quadratic model and the calibrated model using surface emissivity and solar zenith angle is shown in Table 3. The result showed that the correlation between the LST and brightness temperature was increased significantly after the calibration. The determination of coefficient, R^2, increased from 0.33 to 0.85. This indicates that the Landsat TM/ETM+ thermal infrared data can be calibrated using appropriate ground truth and ancillary data.

Coefficients of the models are presented in Table 4, from which the following prediction model was produced.

$$T_G = -1081.4 - 0.43\,T_B^2 + 55.68T_B - 26.76\varepsilon - 9.35\theta \quad (3)$$

Table 3. Model to estimate LST using satellite brightness temperature (1) and calibrated model using emissivity and solar zenith angle (2).

Models	R	R^2	Adjusted R^2	Std. Error of the Estimate
1	.575[a]	.330	.218	2.56
2	.923[b]	.851	.792	1.32

a. Predictors: (Constant), T_B, T_B^2

b. Predictors: (Constant), T_B, T_B^2, ε, θ

Table 4. Coefficients and *t* values of the models.

Models		Unstandardized Coefficients			*t*	Sig.
		B	Std. Error	Beta		
1	(Constant)	-1339.438	1014.247		-1.321	.211
	T_B^2	-.318	.242	-19.911	-1.312	.214
	T_B	42.131	31.354	20.392	1.344	.204
2	(Constant)	-1081.393	537.707		-2.011	.072
	T_B^2	-.428	.140	-26.836	-3.057	.012
	T_B	55.675	18.083	26.947	3.079	.012
	ε	-26.756	58.902	-.075	-.454	.659
	θ	-9.354	1.916	-.853	-4.881	.001

4. Discussion

Many factors affect the retrieval of LST from satellite thermal infrared data but some of them, such as transmittance, air moisture, downwelling and upwelling radiance, are usually difficult to obtain, especially from satellite observations. In this study, we chose only two variables surface emissivity and incoming solar radiation is because they have been demonstrated important in affecting the retrieval of LST from satellite thermal data. The solar zenith angle was used to replace the incoming solar radiation in analysis is because they are highly correlated but solar zenith angle can be calculated easily (Cresswell *et al*., 1999).

R^2 of the calibrated model is much attractive for the real application, much more works need to do in the future to test and modify the model. The *p* value of the surface emissivity in the model is not significant is because several of the weather stations in this study are located on the airports, where the difference of land surface emissivity classes is not significant. We did not remove this variable form the model is because Sutherland and Bartholic (1979) has demonstrated that for an assumed emissivity at the quantity of 1.00, an error of as high as 6 ^{o}C could arise, whereas if an adjustment on emissivity was made, a maximum error could be only

0.8 ^{o}C. In the future, more accurate ground truth temperatures in different 'emissivity classes' collected in northeast United States while Landsat-7 overpass will be applied to test and modify the model. We believe that with more ground truth temperature measured in different 'emissivity classes', the accuracy of the model will be further improved.

In addition to determining the canopy surface temperature, the LST of a forest, ETM+ thermal data can also be used to estimate the temperatures inside a forest, which is impossible with conventional methods. To this end, the vertical profile of temperature (every 6 meters from ground to the canopy) of a mixed forest has being observed since June 2001 on an observing tower in Connecticut by the authors while as Landsat-7 overpasses. This will bring a perspective for the application of satellite thermal data in forestry and landscape research.

In summary, this simple method can be applied to achieve a quick prediction of LST from Landsat ETM+ data with fewer parameters in reasonable accuracy.

Acknowledgement

The research upon which this paper is based was supported by National Aeronautic and Space Administration (NASA) Grant No. NAG5-8829, NAG5-8739, and Rhode Island Agricultural Experiment Station.

Reference:

Becker, F. and Z. L. Li. 1990. Towards a local split window method over land surfaces. *Int. J. Remote Sensing*, 11:369-393.

Cooper, D. I., G. Asrar. 1989. Evaluating atmospheric correction models for retrieving surface temperature from AVHRR over a tall-grass prairie. *Remote Sens. Environ.* 27: 93-102.

Cresswell, M. P., A. P. Morse, M. C. Thomson, and S. J. Connor. 1999. Estimating surface air temperature, form Meteosat land surface temperatures, using an empirical solar zenith angle model. *Int. J. Remote Sensing*, Vol. 20, No. 6, 1125-1132.

Dubayah R. and P. M. Rich. 1995. Topographic solar radiation models for GIS. *Int. of Geographic Information System.* Vol. 9, No. 4, 401-419.

Fitzpatrick, P. (Jackson State University) and G. Stephens (Colorado State University). 1995. Solar Zenith Angle algorithms (source code available from: http://www.liv.ac.uk/~mark/met.htm).

Goetz, S. J., R. N. Halthore, F. G. hall, and B. L. Markham. 1995. Surface temperature retrieval in a temperate grassland with multi-resolution sensors. *Journal of Geophysical research.* Vol. 100, No. D12, 25,397-25,410.

Markham, B. L. and J. L. Barker. 1986. Landsat MSS and TM post-calibration dynamic rangers, exoatmospheric reflectance and at-satellite temperatures. *EOSAT Landsat Tech. Notes* (Aug.): 3-8.

Norman, J. M., J. L. Chen, and N. S. Goel. 1990. Thermal emissivity and infrared temperature dependence of plant canopy architecture and view angle, Proc. 10th Ann. Inter. Geoscience Remote Sensing Symp., Vol. III, pp. 1747-1750. *IEEE*, 445 Hoes Lane, Piscataway, NJ 08854.

Norman, J. M., M. Divakarla, and N. S. Goel. 1995. Algorithms for extracting information from remote thermal-IR observations of the Earth's surface. *Remote Sens. Environ.* 51: 157-168.

Schott, J. R. and W. J. Volchok. 1985. Thematic Mapper thermal infrared calibration. *Photogrammetric Engineering and Remote Sensing*, Vol. 51, No. 9, 1351-1357.

Singh, S. M. 1988. Brightness temperature algorithms for Landsat Thematic Mapper data. *Remote Sens. Environ.* 24: 509-512.

Snyder, W. C., Z. Wan, and Y. Z. Feng. 1998. Classification-based emissivity for land surface temperature measurement from space. *Int. J. Remote Sensing*, Vol. 19, No. 14, 2753-2774.

Sospedra, F., V. Caselles, and E. Valor. 1998. Effective wavenumber for thermal infrared bands—application to Landsat-TM. *Int. J. Remote Sensing*, Vol. 19, No. 11, 2105-2117.

Sutherland, R. A. and J. F. Bartholic. 1979. Emissivity correction for interpreting thermal radiation afrom a terrestrial surface. *J. Appl. Meteorol*. 18:1165-1171.

Vidal, A. 1991. Atmospheric and emissivity correction of land surface temperature measured from satellite using ground measurements or satellite data. *Int. J. Remote Sensing*, Vol. 12, No. 12, 2449-2460.

Wukelic, G. E., D. E. Gibbons, L. M. Martucci, and H. P. Foote. 1989. Radiometric calibration of Landsat Thematic Mapper thermal band. *Remote Sens. Environ. 28*: 339-347.